



Engineering of living autologous human umbilical cord cell-based septal occluder membranes using composite PGA-P4HB matrices

Benedikt Weber^{a,b,1}, Roman Schoenauer^{a,b,1}, Francesca Papadopulos^{b,c}, Peter Modregger^{d,e}, Silvia Peter^{d,f}, Marco Stampanoni^{d,f}, Arabella Mauri^g, Edoardo Mazza^{g,h}, Julia Gorelikⁱ, Irina Agarkova^{a,b}, Laura Frese^{a,b}, Christian Breyman^j, Oliver Kretschmar^k, Simon P. Hoerstrup^{a,b,*}

^aSwiss Center for Regenerative Medicine, University of Zurich, Raemistrasse 100, 8091 Zurich, Switzerland

^bDepartment of Surgical Research and Clinic for Cardiovascular Surgery, University Hospital Zurich, Raemistrasse 100, 8091 Zurich, Switzerland

^cDepartment of Specialistic Surgery and Anesthesiological Sciences, S. Orsola Hospital, University of Bologna, Via Massarenti 9, 40138 Bologna, Italy

^dSwiss Light Source, Paul Scherrer Institute, 5232 Villigen, Switzerland

^eUniversity of Lausanne, School of Biology and Medicine, Rue du Bugnon 21, 1015 Lausanne, Switzerland

^fInstitute for Biomedical Engineering, University and ETH Zurich, ETZ-F-85, Gloriastrasse 35, 8092 Zurich, Switzerland

^gDepartment of Mechanical and Process Engineering, ETH Zurich, Sonneggstrasse 3, 8092 Zurich, Switzerland

^hSwiss Federal Laboratories for Materials Science and Technology, EMPA, Überlandstrasse 129, 8600 Dübendorf, Switzerland

ⁱCardiovascular Sciences, National Heart and Lung Institute, Imperial College London, Dovehouse Street, London, SW36LY, UK

^jFeto-Maternal Haematology Group and Obstetric Research, University Hospital Zurich & GGS Perinatal Center c/o Hirslanden Clinic Zurich, 8091 Zurich, Switzerland

^kDepartment of Pediatric Cardiology, University Children's Hospital Zurich, Steinwiesstrasse 75, 8032 Zurich, Switzerland

ARTICLE INFO

Article history:

Received 13 July 2011

Accepted 25 July 2011

Available online 5 October 2011

Keywords:

Umbilical cord cells
Biodegradable matrix
Septal occluder system
Polyglycolic acid
Poly-4-hydroxybutyrate
Crimping

ABSTRACT

Interventional closure of intracardiac wall defects using occluder devices has evolved as a highly attractive treatment option. However, incomplete and delayed healing reactions often result in a major risk of residual defects, thromboembolism, or device fractures. Biodegradable living tissue engineered occluder membranes (TEOMs) could provide autologous thromboresistant implants with growth and remodeling capacities. PGA-P4HB composite matrices were seeded with human umbilical cord-derived cells or vascular-derived control cells and exposed to static ($n = 19$) or dynamic ($n = 13$) conditioning. Harvested TEOMs were integrated into occluder frameworks, exposed to crimping and delivered into pre-formed defects of juvenile porcine hearts. Dynamically conditioned TEOM constructs showed higher collagen formation in histology than static constructs with significantly higher stiffness moduli in uniaxial tensile testing. Grating interferometry revealed substantial but inhomogeneous cone-like degradation of the composite matrices in dynamic conditioning. The crimping and delivery procedures resulted in no significant changes in macroscopy, histo-morphology, cellular viability, DNA or hydroxyproline content, and scanning electron microscopy findings. Here, we present the in vitro fabrication, crimping and experimental delivery of living human umbilical cord-cell derived TEOMs based on composite matrices as a potential future autologous therapy of intracardiac wall defects.

© 2011 Elsevier Ltd. All rights reserved.

1. Introduction

In recent years interventional closure of intracardiac wall defects has evolved as a highly attractive alternative treatment to surgical correction by preventing thoracotomy and cardiopulmonary bypass [1–3]. For occlusion of the defects several different

interventional devices have been developed [2]. In spite of the evident differences in the outer implant design, all devices comprise a metallic frame or meshwork and synthetic polymer membranes. After deployment, the devices encounter a natural foreign body response with transanastomotic tissue ingrowth and coverage [3–5]. However, often these healing reactions are characterized by incomplete and delayed incorporation of devices into the cardiac tissue, which results in a major risk of residual intracardiac defects, associated infections, thromboembolism, friction lesions or fractures with device embolization [3,5]. In addition, considering that these devices are implanted into young infants with in principle high life expectancies, the potential long-term

* Corresponding author. Swiss Center for Regenerative Medicine, University of Zurich, Raemistrasse 100, 8091 Zürich, Switzerland. Tel.: +41 44 255 3644; fax: +41 44 255 4369.

E-mail address: simon_philipp.hoerstrup@usz.ch (S.P. Hoerstrup).

¹ These authors contributed equally to the work.

consequences related to the implantation of foreign body material into a dynamically moving and growing heart for their cardiac development and later adult cardiac functionality remains to be elucidated. After interventional closure of the defect and coverage by a continuous layer of endogenous tissue, the synthetic implants are no longer necessary. Conversely, the synthetic device materials lack the ability to grow with the developing infant's heart and may be potentially harmful for the recipients' cardiac development and/or functionality [3,6].

Tissue engineered living septal occluder membranes based on fully biodegradable scaffold materials together with biodegradable frame meshes could overcome these limitations by combining robust, thromboresistant surfaces with fully biodegradable device properties as well as an optimal healing environment with growth potential composed of autologous vascular cells. The concept for cardiovascular tissue engineering has been proven for heart valves [7–13] and vascular grafts [13–15] by a series of studies involving the *in vitro* fabrication as well as the experimental [16,17] and initial clinical [18,19] *in vivo* investigation. For pediatric applications fetal progenitor cells have proven to be a promising autologous cell source [20–22]. In particular umbilical cord-derived cells have gained significant attention as a unique autologous perinatal cell source used to fabricate these constructs [23–26]. Importantly, they do not only show favorable growth properties, they also have a high clinical relevance due to their high accessibility and lack of

additional cell harvest procedures [27]. The main focus of tissue engineered heart valve- and vessel-development was the generation of native-like cardiovascular structures with proper functionality. Tissue engineered occluder membranes (TEOMs) would require not only constructs with high mechanical resilience, but also constructs that can undergo a strenuous crimping procedure without significant cellular loss and/or bioengineered matrix laceration in order to survive the harmful delivery procedures of today's minimally invasive interventional routes.

Here, we investigate the *in vitro* fabrication, crimping analysis as well as experimental delivery of living human umbilical cord-cell derived tissue engineered septal occluder membranes based on composite matrices as a potential future autologous therapy of intracardiac wall defects.

2. Materials and methods

2.1. Cell harvest and isolation

Human umbilical cord cells were harvested as previously described [24–26]. After informed consent was obtained from the participants (approved by the Ethics Committee [STV-95-2009]) fresh human umbilical cord tissue of healthy individuals was collected. Briefly, human umbilical cord tissue obtained from Wharton's jelly by excision biopsy was minced into pieces of approximately 8 mm³ and placed into culture dishes. Outgrowing umbilical cord-derived mesenchymal cells were expanded up to the eighth passage in advanced DMEM (Invitrogen, Life Technologies, USA). Mature vascular-derived control cells were obtained from the vena

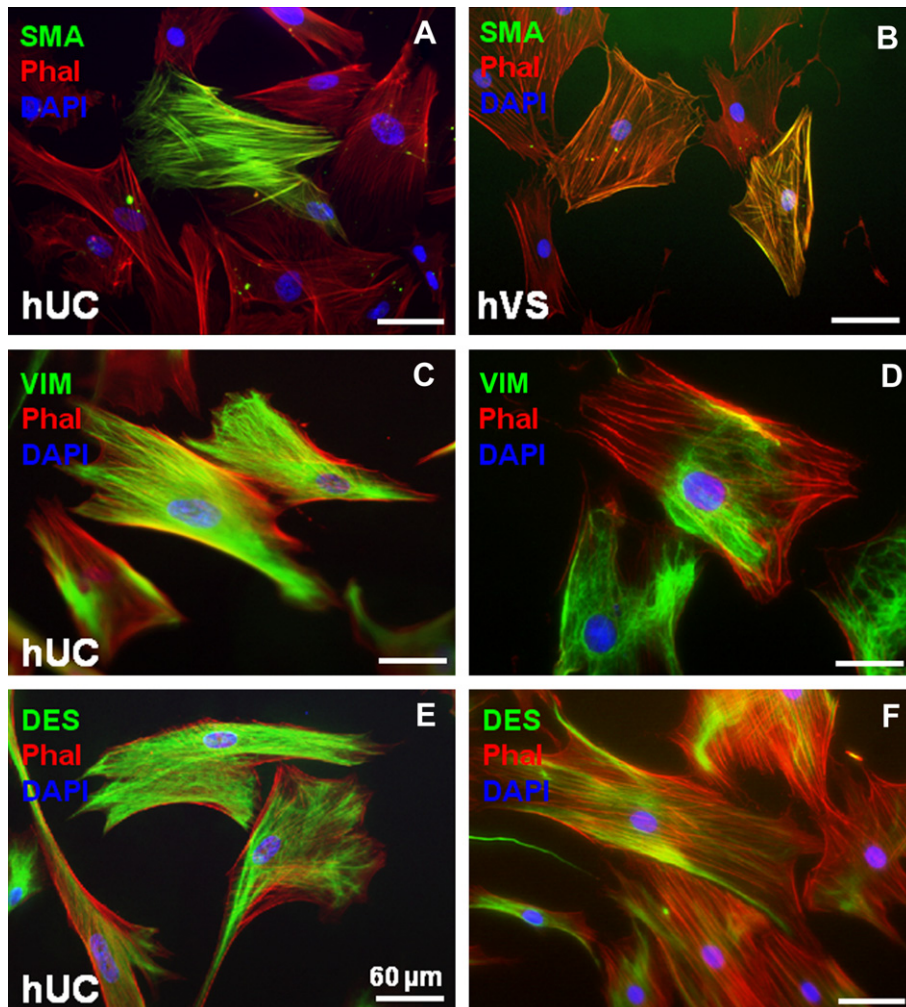


Fig. 1. Cellular phenotypes. Human umbilical cord Wharton's jelly-derived cells revealed smooth muscle-like phenotypes with positive stainings for vimentin (C), desmin (E) and partially for α -sma (A) similar to mature vascular-derived myofibroblasts (B, D, F).

saphena [KEK-STV-21-2006]. All media were supplemented with 100 IU/l penicillin and 10 mg/l streptomycin (P 0781; Sigma-Aldrich, St. Louis, USA), 10% Fetal Bovine Serum (Invitrogen, Life Technologies, USA) and 2,5 mg/l Fungizone (Sigma-Aldrich, St. Louis, USA).

2.2. Umbilical cord-derived endothelial cells

Human umbilical cord vein-derived endothelial cells (HUVEC) were isolated using a collagenase installation technique. The umbilical cord veins were incubated in 0.2% collagenase (Collagenase A, Roche Diagnostics GmbH, Mannheim, Germany) dissolved in serum-free medium (EGMTM-2; Lonza Group AG, Basel, Switzerland). After 20 min, the cell suspension was centrifuged. Cells were cultured and expanded in EGM-2 medium (EGMTM-2) containing growth factors and supplements (vascular endothelial growth factor, human fibroblasts growth factor, human recombinant long-insulin-like growth factor-1, human epidermal growth factor, gentamicin and amphotericin, hydrocortisone, heparin, ascorbic acid, and 2% fetal bovine serum).

2.3. Phenotyping of cells

Isolated cells were characterized using immunofluorescence staining. Primary antibodies used for characterization of cells were against α -smooth muscle actin (mM-

anti-human, clone 1A4, Sigma–Aldrich, St. Louis, USA), desmin (mM-anti-human desmin, clone D33, DakoCytomation, Copenhagen, Denmark), vimentin (mM-anti-human vimentin, clone Vim 3B4, DakoCytomation, Copenhagen, Denmark), CD31 (mM-anti-human CD31, clone JC70A, DakoCytomation, Copenhagen, Denmark), and von Willebrand factor (pR-anti-human von Willebrand factor, DakoCytomation, Copenhagen, Denmark). Alexa 633 phalloidin and DAPI were used as control staining (Invitrogen, Life Technologies, USA). Primary antibodies were detected with Cy-2 or Cy-3 goat-anti-mouse and Cy-5 goat-anti rabbit antibodies (Jackson ImmunoResearch Laboratories Inc., West Grove, PA). For immunostainings cells were first washed with PBS and then fixed with 4% paraformaldehyde in PBS for 10 min. Following a second washing phase (PBS), they were blocked with 0.1 M glycine in PBS for 5 min and permeabilized in 0.2% Triton X-100/PBS for 10 min. After blocking with 5% goat serum and 1% bovine serum albumin in PBS for 1 h, primary antibodies were added and incubated for 1 h at room temperature. After three washing steps with PBS (5 min), secondary antibodies were added for 45 min. The specimens were washed again three times in PBS for 5 min and mounted in 0.1 M Tris–HCl, pH 9.5, and glycerol (3:7) containing 50 mg/mL of *n*-propyl gallate as anti-fading reagent.

Analysis of the stained sections and cells was carried out using an inverted fluorescence microscope equipped with a CCD camera (Leica Microsystems AG, Heerbrugg, Switzerland). Image processing was performed using the Leica Application Suite processing software (Leica Microsystems AG, Germany) and PhotoShop (Adobe Systems, San Jose, CA).

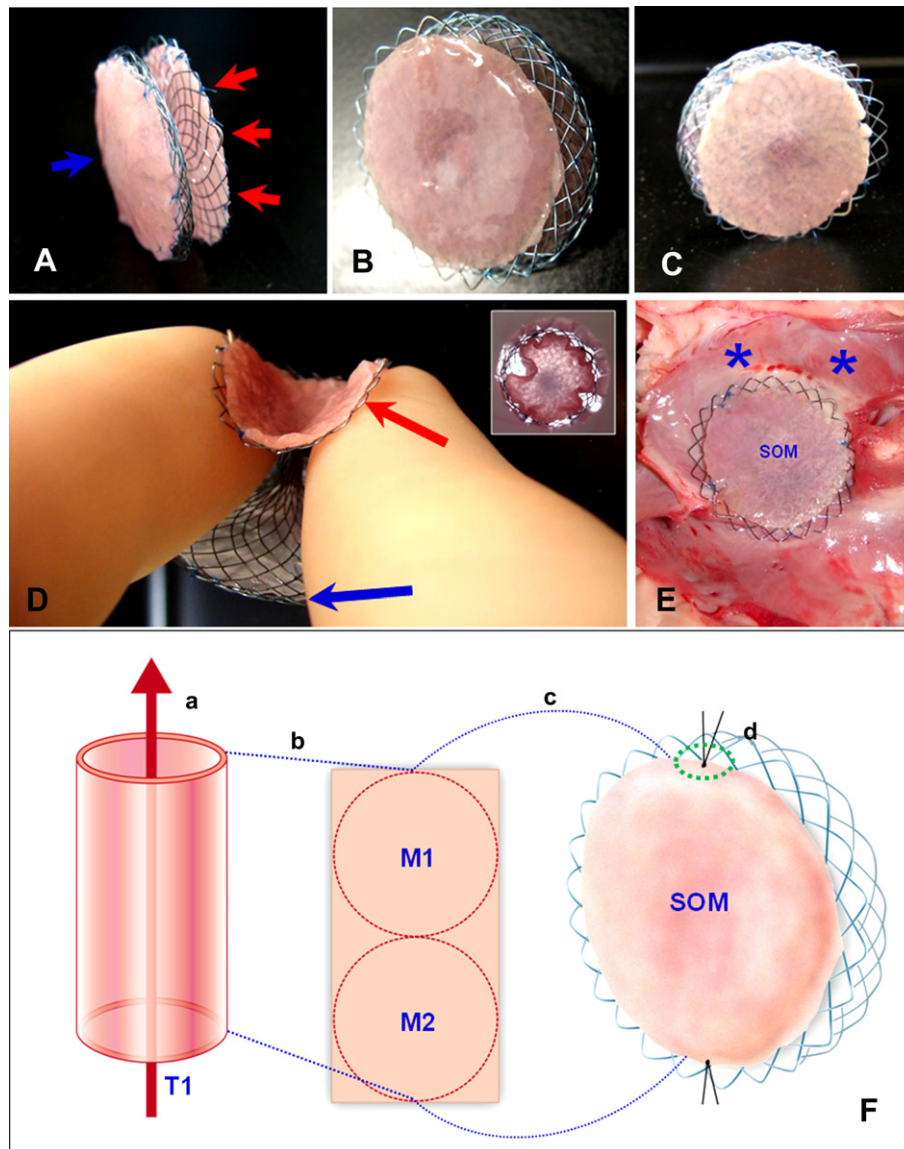


Fig. 2. Fabrication and delivery of TEOMs. After dynamic in vitro conditioning, the constructs (A–E) were excised from the deriving bioengineered sheets (Fa and b) and attached to the metallic frame of the occluder devices (A–C, arrows indicate TEOM constructs on both occluder sides; F,c and d) for crimping (D, arrows) and delivery (E, *inter-atrial septum; SOM = septal occluder membrane).

2.4. Scaffold fabrication

Tube like-shaped matrices were fabricated from non-woven polyglycolic acid meshes (PGA; thickness 1.0 mm; specific gravity 70 mg/cm³; Cellon, Luxembourg), coated with 1.75% poly-4-hydroxybutyrate (P4HB; MW: 1×10⁶; TEPHA Inc., USA) by dipping into a tetrahydrofuran solution (THF; Fluka, Germany). After solvent evaporation, physical bonding of adjacent fibers and continuous coating was achieved. P4HB is a biologically derived rapidly degradable biopolymer, which besides being strong and pliable is thermoplastic (61 °C), and can be molded into three-dimensional shapes. From the PGA-P4HB composite scaffold material, the septal occluder matrices were fabricated by integrating the scaffold into a nitinol frame that was fixated in a Plexiglas-tube for positioning in the biomimetic flow system (length = 29.5 ± 0.6 mm; OD = 20.2 ± 1.6 mm, pfm AG, Germany). This connection was achieved by attaching the scaffold matrix to the inner surface of the nitinol frame using single interrupted sutures (5–0 Polypropylene, Ethicon, USA). After vacuum drying for 24 h, the scaffolds were sterilized overnight by using ethylene oxide (EtO) gas sterilization. The EtO was allowed to evaporate for 3 days and the scaffolds were incubated in DMEM medium (Sigma-Aldrich, St. Louis, USA) for 24 h to facilitate cell attachment by deposition of proteins. All media were supplemented with 10% fetal bovine serum (Sigma-Aldrich, St. Louis, USA), 0.05% Pen/Strep (P 0781; Sigma-Aldrich, St. Louis, USA) and 2.5 mg/L Fungizone (Sigma-Aldrich, St. Louis, USA), adjusted to a pH of 7.4, buffered with NaHCO₃ (Sigma-Aldrich, St. Louis, USA) and sterilely filtered.

2.5. Cell seeding

Wharton's jelly myofibroblasts (WMFs) were seeded onto composite matrices (1.5 (*n* = 2) up to 3.0 (*n* = 7) × 10⁶ cells/cm² scaffold) using fibrin (Sigma-Aldrich, St. Louis, USA) as a cell carrier. The concentration of Fibrinogen (10 mg/mL) and Thrombin (10 IU/mL) was in accordance with the standard concentrations used in cardiovascular tissue engineering [28]. After static incubation of seeded constructs in advanced DMEM (Sigma-Aldrich, St. Louis, USA; 10% FBS; P/S supplement) for four days, they were placed into a bioreactor flow system mimicking a pulsatile pressure cardiovascular flow environment. The pulsatile flow was slightly increased over the study period and DMEM medium was changed every 3–4 days. Constructs were harvested after 7 and 14 days of biomimetic conditioning accordingly. For endothelialization constructs were seeded with 1.0 × 10⁶ cells/cm² membrane and

constructs were cultured for 2 additional days in EGM-2 medium (EGMTM-2; Lonza Group AG, Basel, Switzerland; Medium B constructs).

2.6. Histological analysis

Qualitative analysis of tissue engineered constructs was performed using histology and immunohistochemistry by H&E staining, Masson Trichrome staining and stainings for α -smooth muscle actin (clone 1A4, Sigma-Aldrich, St. Louis, USA). Sections were analyzed using an inverted light microscope and compared to native tissues.

2.7. Grating interferometry

PGA-P4HB matrices as well as bioengineered constructs (*n* = 2) were evaluated using grating interferometry (GI). GI represents an X-ray imaging method that exploits phase information in addition to absorption contrast. The experiments were performed at the TOMographic Microscopy and Coherent rAdiology experiments (TOMCAT) beamline of the Swiss Light Source (Paul Scherrer Institute, SLS, Villigen, Switzerland [29]). A photon energy of 25 keV was selected by a double multilayer.

The experimental setup consisted of a phase grating downstream of the sample that provides a rectangular-shaped interference pattern at the Lohmann distance (here: 121 mm) [30]. At the position of the interference pattern an absorption grating is used to analyze local lateral offset of the pattern, which are proportional to the first derivative of the phase shift caused by the sample. This is done by laterally scanning one grating with several steps over a fraction of the pitch of the absorption grating and then analyzing the pixel-wise intensity distributions by a Fourier-based approach [31].

The samples were embedded in 2% agarose gel within an Eppendorf cylinder for mechanical fixation. The tomography scan was performed with 1601 projections over 180° and 8 phase steps over 2 periods. The total scan time was approximately 1.5 h. Multi-slice information was combined in three-dimensional images and different stages of the TEOM constructs were compared.

2.8. Quantitative tissue analysis

Septal occluder membranes were minced, lyophilized, and analyzed by biochemical assays for total DNA content as an indicator for cell number,

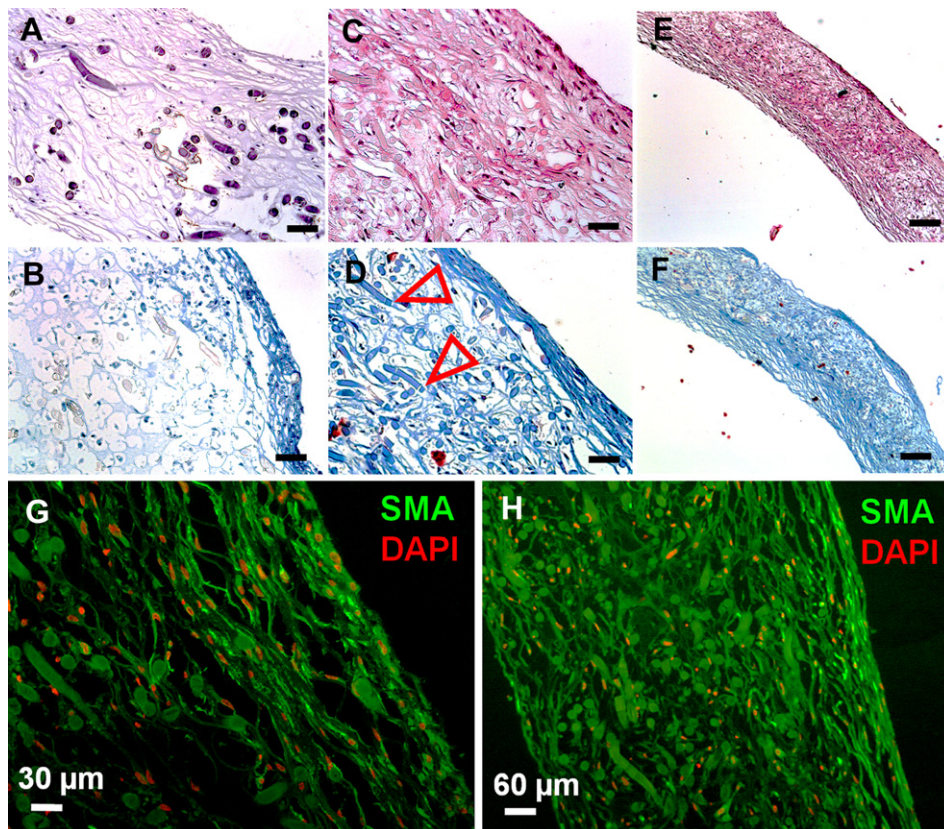


Fig. 3. Microscale analysis of bioengineered occluder membranes. Static constructs (A: H&E, B: Masson Trichrome, A–D: scale bar ~60 μm) showed substantially lower collagen formation in direct comparison to dynamically cultured constructs (C and E: H&E; D and F: Masson Trichrome; E–F: scale bar ~120 μm). Both, static and dynamic constructs, showed remnant PGA-P4HB scaffold material in histology. In dynamically conditioned TEOMs, a pronounced α -SMA positive layer was detectable (G–H).

hydroxyproline (HYP) content as an indicator for collagen, as well as for glycosaminoglycans (GAG) content. For measuring the DNA amount, the Hoechst dye method [32] was used with a standard curve prepared from calf thymus DNA (Sigma-Aldrich, St. Louis, USA). The GAG content was determined using a modified version of the protocol described by Farndale et al. [33] and a standard curve prepared from chondroitin sulfate derived from shark cartilage (Sigma-Aldrich, St. Louis, USA). HYP was determined with a modified version of the protocol described by Huszar et al. [34].

2.9. Biomechanical analysis

The mechanical properties of the TEOMs were determined in triplicate by uniaxial tensile tests. The TEOMs were cut along their axis and spread out in order to generate samples. These samples were cut in longitudinal direction with a cutting tool made of razor blades separated with 2 mm spacer blocks. The dimension of the samples was of approx. 2 mm × 20 mm. The tensile tests were performed on a custom-built miniature tension machine. This mechanical test setup consists of a linear horizontal motor (PI M-505 4PD, Physik Instrumente GmbH, Germany) and a 10 N load cell (force transducer KAW-S, AST Mess- & Regeltechnik, Germany). The whole experimental setup was controlled by a LabView (LabView, National Instruments, USA) program code.

The samples were mounted in two parallel clamps with an initial chuck width of 12 mm. The interior of the clamps was coated with sandpaper to improve soft-tissue gripping. After preconditioning of ten cycles, monotonic strain to failure tests were performed under displacement controlled conditions, with a displacement rate of 0.12 mm/s which corresponds to an elongation rate of 1% nominal strain per second. The force-displacement data were sampled with a frequency of 15 Hz and were afterward converted into tension-strain curves. The nominal strain values were calculated by dividing the current length of the samples by their initial length and subtracting 1. The accurate width was determined for each sample by image analysis. Nominal tension values (measured force divided by the initial width of the sample) were preferred to the nominal stress values because of the inhomogeneous thickness of the material.

2.10. Simulated delivery and crimping analysis

For evaluation of the effect of the delivery procedure on the structural integrity of autologous bioengineered septal occluder membranes ($n = 3$), tissue engineered constructs were delivered experimentally into pre-formed interatrial septum defects of porcine juvenile hearts ex vivo. For this purpose, engineered membranes were crimped by folding along the axial sheath axis to a radial diameter of 5.0–8.0 mm. The engineered constructs were left in crimped state for 15 min at 25 °C, which represents a clinically relevant time frame. After delivery, the effects of crimping on tissue integrity of the bioengineered membranes and on cell viability were analyzed by histology, immunohistochemistry, life-dead assay (LIVE/DEAD® Viability/Cytotoxicity Kit, Invitrogen, Life Technologies, USA) and biomechanical assays and compared to non-crimped control constructs.

2.11. Live dead assay

Analysis of cell viability was performed by using a life-dead assay ($n = 6$; LIVE/DEAD® Viability/Cytotoxicity Kit, Invitrogen, Life Technologies). This assay discriminates live from dead cells by simultaneous staining with green-fluorescent calcein to indicate intracellular esterase activity and red-fluorescent ethidium homodimer to indicate loss of plasma membrane integrity. The samples were analyzed directly after staining under the confocal microscope (Leica SP5, Leica Microsystems, Heerbrugg, Switzerland). Image processing was performed by using the Leica Application Suite (Leica Microsystems) and Photoshop (Adobe Systems, San Jose, CA). Quantification of the calcein signal was performed by ImageJ (Image 1.44p, NIH, USA).

2.12. Scanning ion conductance microscopy (SICM)

SICM allows high-resolution, non-invasive probing of the surface of unfixed living cells and was used for identification of cellular crimping effects on the engineered construct surfaces. Briefly, the pipette mounted on a piezo stage is moved over the cell while maintaining a fixed distance from the surface. This is achieved by a feedback control keeping the ion current flowing through the pipette to the cell surface constant. The glass nanopipette is a sensitive probe that detects ion current and uses the current as an interaction signal to control the vertical (z -axis) position of the cell relative to the pipette tip. In our experiments we used hopping probe ion conductance microscopy (HPICM) without continuous feedback [35,36]. Instead, at each imaging point, the pipette approaches the sample from a starting position that is above any of the surface features. The reference current is measured while the pipette is well away from the surface. The pipette then approaches until the current is reduced by a pre-defined amount, usually 0.25–1%. Typically, even at a 1% reduction of the current, the pipette is still at a distance of about one inner pipette radius from

the surface. The z -dimension actuator then withdraws the pipette away from the surface and the sample is moved laterally to the next imaging point. By continuously updating the reference current while the pipette is away from the surface, the method automatically adjusts for any slow drifts in the pipette current. SICM analysis was performed on samples of minor manipulation, major manipulation as well as untreated control samples.

2.13. Statistical analysis

Quantitative data are presented as mean ± standard deviation. For statistical comparison of the ECM and the live dead results a Mann–Whitney U test was performed. For analysis of biomechanical data a student's t -test was used. All P -values were two-tailed and a $P < 0.05$ was considered statistically significant (SPSS Inc., Chicago, IL, USA).

3. Results

3.1. Morphology and phenotype of isolated cells

Outgrowing Wharton's jelly myfibroblasts (WMFs) expressed high levels of vimentin and desmin (Fig. 1C and E). α -smooth muscle actin was only partially expressed in expanded WMFs (Fig. 1A). This morphology and staining pattern of surface markers is characteristic for smooth muscle-like cells and reflects a phenotype comparable to myfibroblasts isolated from the saphenous vein (Fig. 1B, D and F).

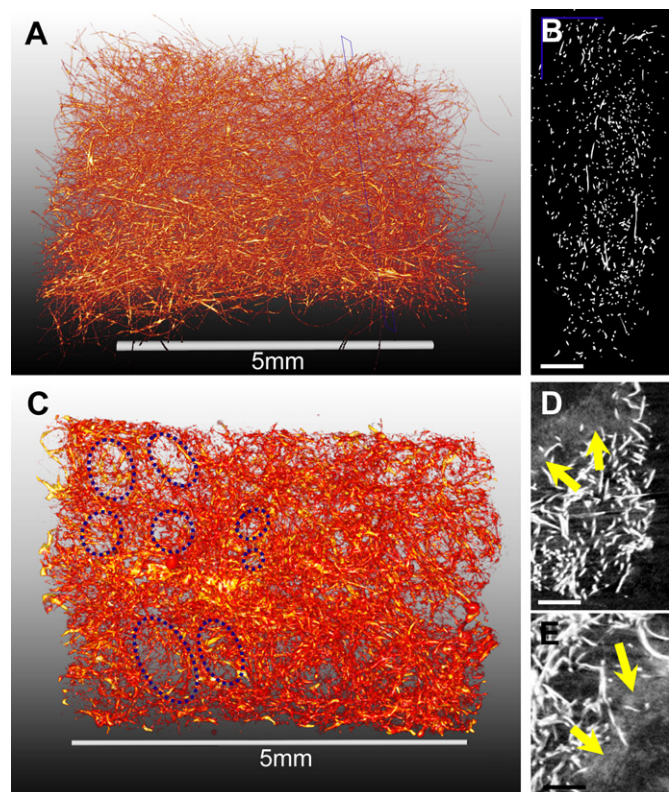
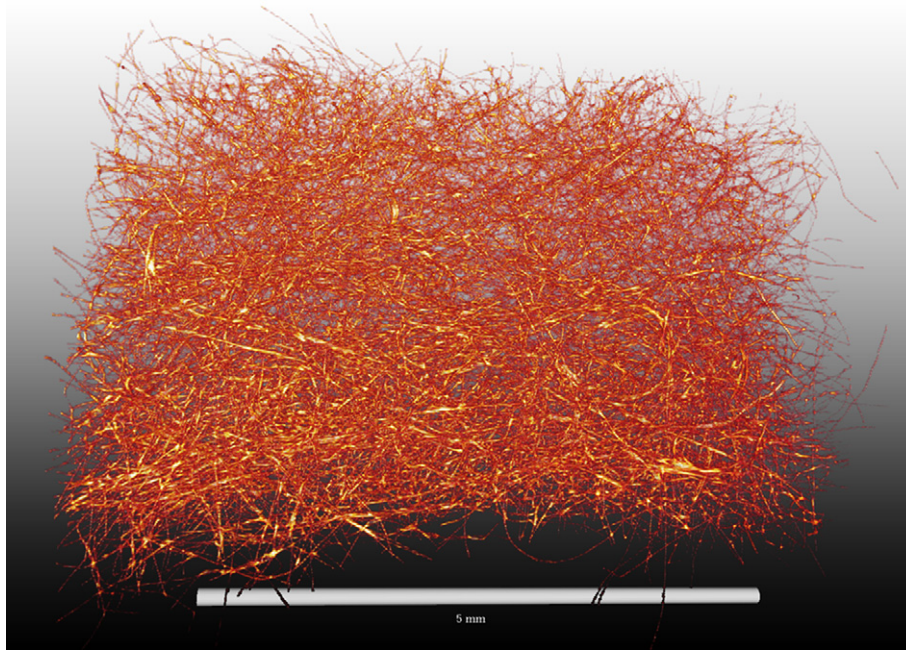


Fig. 4. Grating interferometry 3D microscale analysis. Before dynamic conditioning TEOMs showed a dense composite scaffold meshwork in GI-reconstruction (A) and in slice images (B, scale bar ~400 μm). In the contrary, dynamic constructs revealed clear but inhomogeneously distributed zones of scaffold degradation (C, blue circles) with a cone-like formation of these degradation zones after three weeks in the flow bioreactor (C). Between the degraded PGA-P4HB meshwork zones of neo-tissue were visible (D and E; yellow arrows; scale bar ~200 μm). (For interpretation of the references to color in this figure legend, the reader is referred to the web version of this article.)

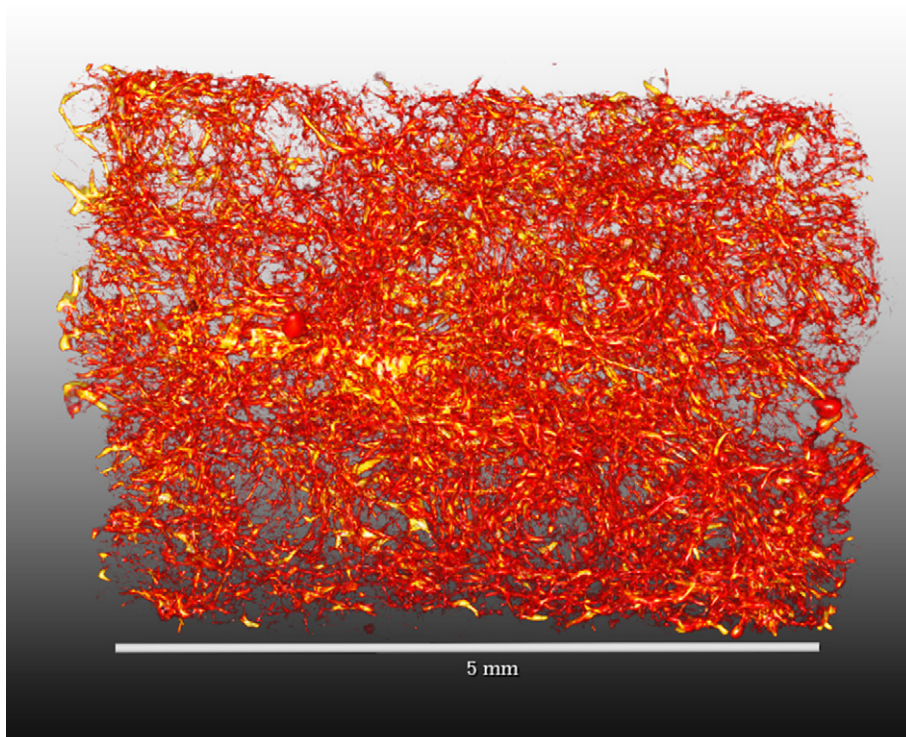


Video 1.

3.2. Analysis of the bioengineered septal occluder membranes: macroscopic appearance

After successful isolation, WMFs were expanded and seeded onto composite scaffolds for dynamic conditioning for 18 ($n = 5$) or 24 ($n = 4$) days. Saphenous vein-derived control constructs were treated equally and conditioned for 18 days ($n = 4$). Control constructs were cultured under static environment and harvested accordingly ($n = 19$). The conduit-like constructs were intact and

pliable (Fig. 2A) with neo-tissue densely covering the bioengineered tubes independent of the conditioning protocol used. Circular membranes could be successfully excised from the conduits and attached to the occluder device framework without macroscopic laceration of the constructs (Fig. 2B and C). Excised TEOM constructs could then be successfully used for crimping analysis (Fig. 2D) and simulated delivery (Fig. 2E). A detailed illustrative explanation of the TEOM fabrication steps is provided in Fig. 2F.



Video 2.

3.3. Histology and immunohistochemistry

Tissue engineered occluder membranes (TEOMs) grown under static conditions (control constructs) demonstrated cellular ingrowth but little tissue formation in H&E staining (Fig. 3A) and little production of extracellular matrix (ECM) with Trichrome-Masson-staining (Fig. 3B). In contrast, constructs of all bioreactor groups (18/24d) showed substantial tissue formation with production of ECMs (Fig. 3C–F). In detail, Trichrome-Masson-staining highlighted collagen formation at the outer layers (Fig. 3D and F), whereas in the center, loosely arranged ECM with scaffold remnants was detectable (Fig. 3D, arrows represent residual scaffold). α -SMA positive cells were present in superficial layers of both, static and dynamic, constructs. However, in dynamically conditioned TEOMs the α -SMA positive layer was more pronounced and deeper (Fig. 3G and H).

3.4. Grating interferometry

For three-dimensional analysis of in vitro tissue formation and degradation of the composite matrix grating interferometry (GI) was performed before and after dynamic conditioning of the TEOM constructs. In comparison to the unconditioned constructs (Fig. 4A and B, Video 1), the conditioned TEOM samples (Fig. 3C–E, Video 2) revealed clear tissue formation embedded into remnants of the PGA-P4HB scaffold meshwork. The signal for the composite scaffold was reduced after 14 days of dynamic conditioning suggesting degradation of the composite matrix components as confirmed by histology (Fig. 3A–D). Interestingly, in the three-dimensional GI-reconstruction this scaffold degradation was not homogeneously distributed but revealed cone-like formations of almost completely degraded zones (Fig. 4C, blue circles) versus areas with full matrix integrity indicating a cluster-like tissue maturation within the bioengineered TEOMs.

3.5. Biomechanical properties

To characterize the biomechanical performance of TEOMs after static and dynamic conditioning, representative samples were analyzed using uniaxial tensile testing. While tension–strain curves of the PGA-P4HB composite matrix showed a steep increase of tension with higher strain, tension–strain behavior of TEOMs approximated to that of native reference tissue (Fig. 5A). However, despite this general similarity, the stiffness of native tissue was substantially lower than in bioengineered membranes indicated by only a slight increase in tension for higher strains as characteristic for native biological material. When comparing the tangential stiffness moduli at high strain [HS-Modulus (HSM); High strain stiffness: N/mm], the HSM of dynamically conditioned samples (24d; $n = 3$) was significantly higher than the HSM of statically conditioned samples ($P = 0.012$; Fig. 5B). This implies that the biomimetic conditioning increases the high strain stiffness of the TEOMs due to evolving tissue formation. Interestingly, also culturing of dynamically conditioned constructs in EGM-2 after endothelialization resulted in a significant decrease of high strain stiffness. In addition, the PGA-P4HB composite matrix showed anisotropic tension–strain behavior in longitudinal versus circumferential direction ($P = 0.017$; high strain stiffness) and all results were presented in consideration of this intrinsic matrix anisotropy (Fig. 5C).

3.6. Crimping analysis – macroscopy and histology

TEOMs were crimped in a custom-made crimping device, introduced into a delivery system and deployed into pre-formed

atrial septal defects of porcine juvenile hearts. Histological analysis after crimping and simulated delivery included comparison after crimped ($n = 4$) versus uncrimped ($n = 4$) TEOMs is shown in Fig. 6A–F. H&E as well as Trichrome-Masson-staining revealed integrity of the α -SMA positive luminal collagen layer after crimping and simulated delivery. No signs for impairment of the constructs' integrity on the histological level, such as holes or fractures, could be identified. Also macroscopically no signs of impairment or inhomogeneity could be identified. However, in histology the impression of a distinct compaction of the TEOM constructs during crimping could be seen when compared to the uncrimped controls of the same conduit patch (Fig. 6E and F).

3.7. Crimping analysis – scanning electron microscopy

After crimping and simulated delivery TEOM surfaces were analyzed using scanning electron microscopy (SEM). In SEM the cell arrangement corresponded to the flow direction of the dynamic flow environment of the bioreactor (Fig. 6G–J). Similar to histology, also SEM revealed no structural impairment, such as cracks or holes, of the crimped construct surfaces (Fig. 6H and J). In addition, no changes on the cellular level on the construct surfaces could be identified.

3.8. Crimping analysis – viability

In order to assess the cellular viability of the TEOMs throughout the crimping procedure, samples of crimped and uncrimped constructs were analyzed using a cell viability assay and quantified using confocal microscopy-based fluorescence quantification ($n = 6$). When directly comparing crimped versus uncrimped samples of the same conduit no significant changes in cellular viability could be identified ($P = 0.19$; Fig. 7A, C and G). Moreover, no

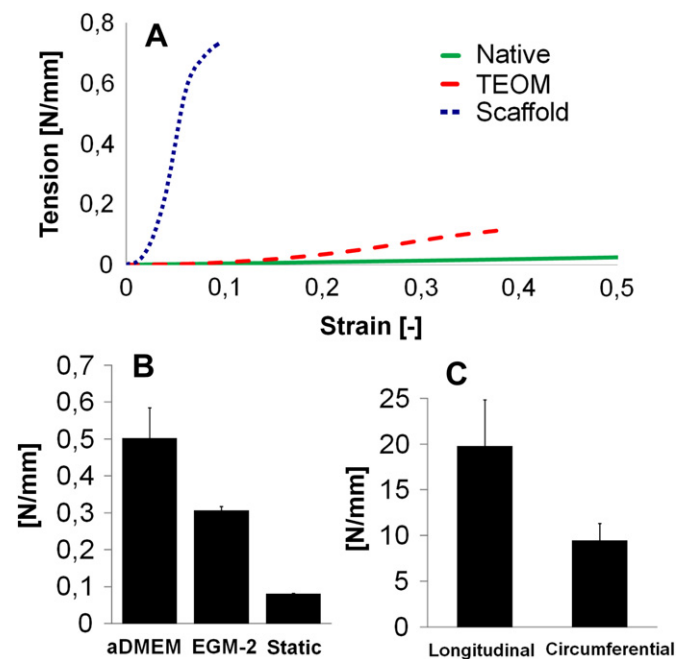


Fig. 5. Biomechanical properties of dynamic TEOM constructs (TEOM: A–B) were compared to native tissue (native) and the PGA-P4HB scaffold alone (scaffold) (A). Tangential stiffness moduli at high strain revealed a significant difference between statically conditioned samples (static), dynamically conditioned samples (aDMEM) and dynamically conditioned constructs cultured in EGM-2 after endothelialization (EGM-2, B). The composite scaffolds were characterized in longitudinal and circumferential direction to detect intrinsic anisotropy and the tension–strain curves were compared (C).

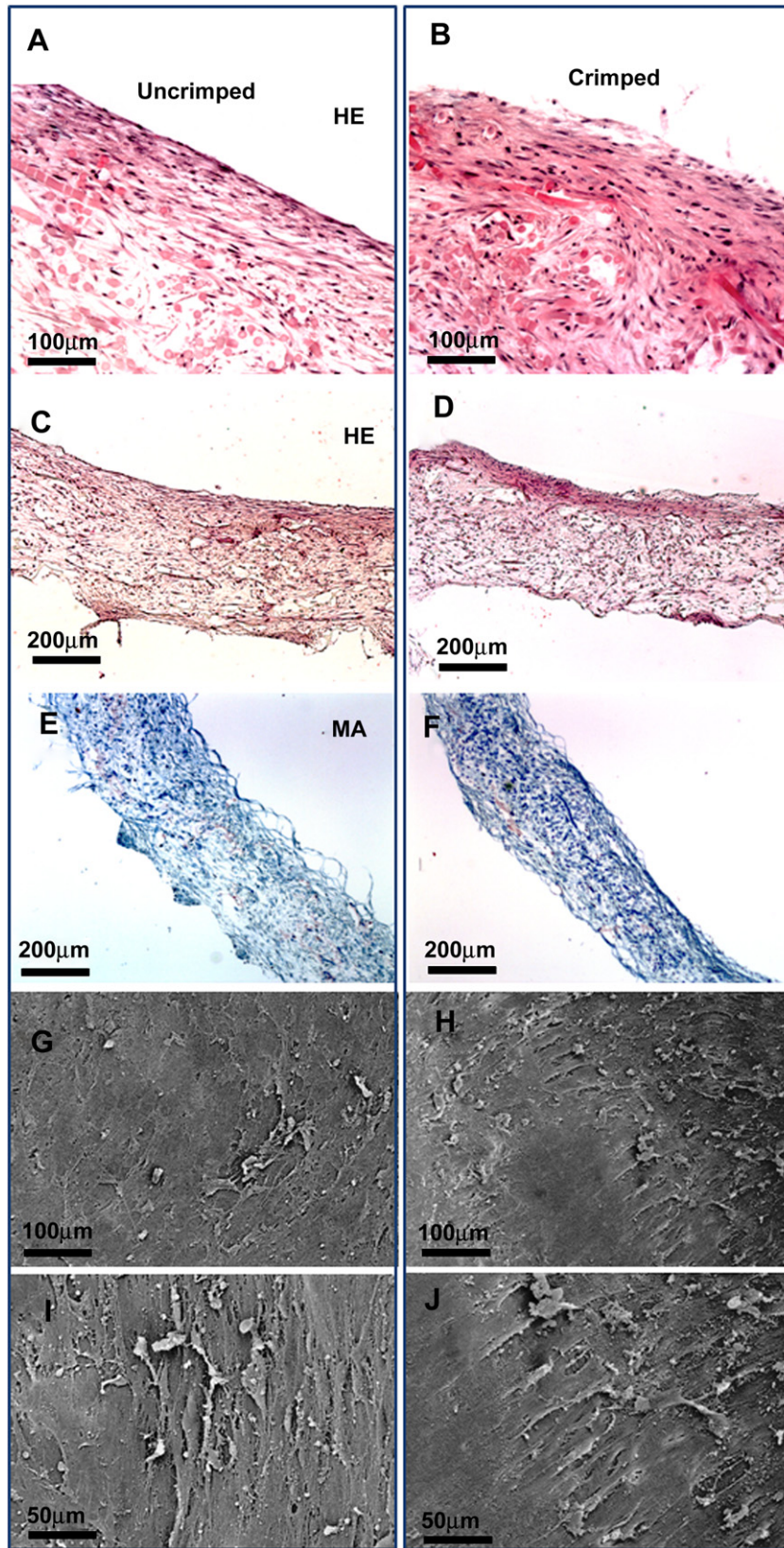


Fig. 6. Crimping analysis. TEOMs were crimped and compared to uncrimped reference samples using H&E stainings (A–D), Masson Trichrome stainings (E and F) and SEM surface analysis (G–J).

differences were seen when comparing constructs based on umbilical cord-derived WMFs with TEOMs based on mature vascular-derived cells (Fig. 7A–D). In contrast, Triton-X 100 pre-treated TEOM samples revealed lack of viable cells within the constructs and served as negative controls with significant decrease in fluorescence (vs. untreated samples $P < 0.025$; Fig. 7E–G).

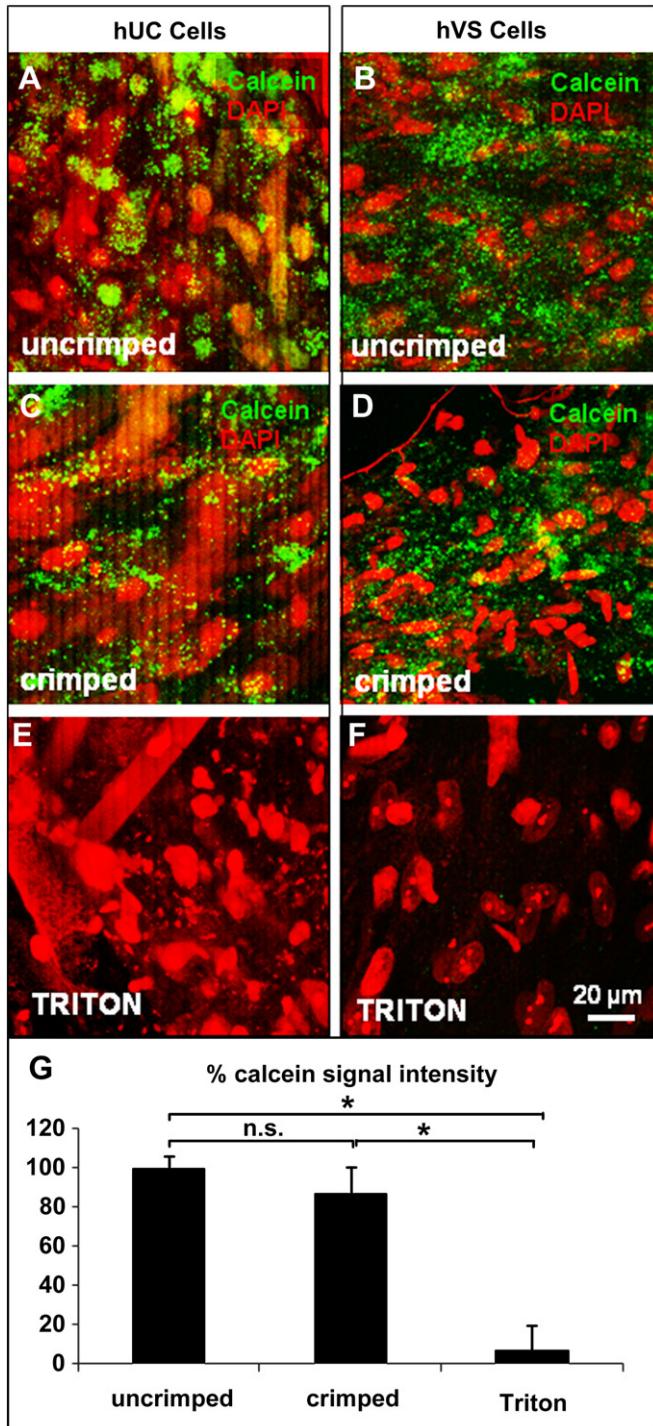


Fig. 7. Cell viability after crimping. Bioengineered occluder membranes based on human umbilical cord cells (hUC cells; A) and human vena saphena-derived control cells (hVS cells; B) were crimped and analyzed using live-dead assay (C and D). Triton-X 100 pre-treated samples served as negative controls (E and F). Fluorescence signal intensity of crimped versus uncrimped samples showed no significant differences (G; n.s. = not significant; * significant for the $P < 0.05$ -level corrected for Bonferroni).

3.9. Crimping analysis – extracellular matrix analysis

For qualitative assessment of TEOM samples extracellular matrix (ECM) analysis for determination of DNA, glycosaminoglycans (GAG), hydroxyprolines (HYP) was performed before and after crimping. After crimping DNA values were not significantly different from values before crimping ($P = 0.91$; Fig. 8A). The amount hydroxyprolines (HYP) per μg tissue slightly increased during the crimping procedure (Fig. 8C). However, the differences were not significant ($P = 0.61$) and may represent an artifact of the tissue compaction reported above. For the glycosaminoglycan (GAG) content per μg tissue no significant changes were seen after the crimping procedure ($P = 0.11$; Fig. 8B).

3.10. Crimping analysis – SICM

For identification of crimping-related destruction on the endothelial cell level scanning ion conductance microscopy (SICM) was performed before (Fig. 9A) and after manipulation of unfixed representative samples of TEOMs ($n = 3$, static constructs). After a first crimping phase involving minor manipulation of the constructs, no effects of the crimping procedure could be identified on the SICM level. However, after a pronounced crimping, involving compression by a metallic device, clear destructive cell borders could be identified by SICM in the region of the maximum exposure confirming the principal feasibility of SICM for detection of cellular crimping effects on bioengineered surfaces (Fig. 9B,C).

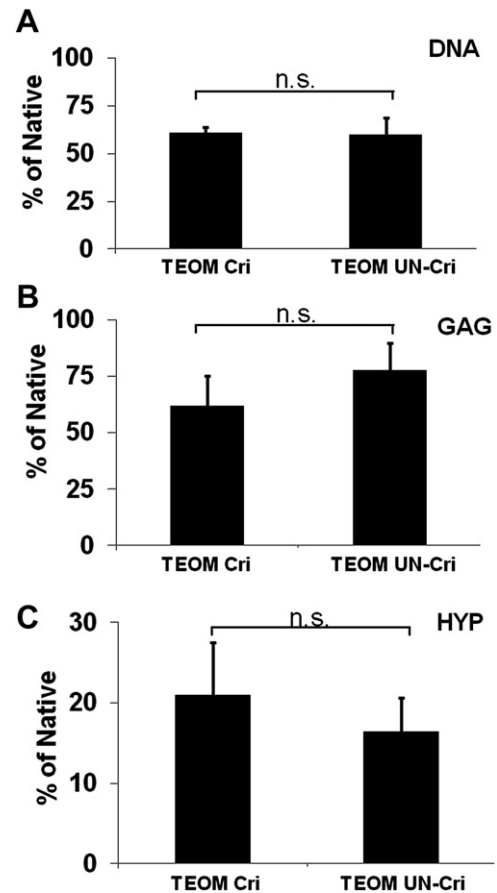


Fig. 8. Extracellular matrix changes during crimping. The contents of DNA (A), glycosaminoglycans (GAG; B) and hydroxyprolines (HYP; C) were measured before and after crimping of TEOM constructs and compared (n.s. = non significant; * significant for the $P = 0.05$ -level).

4. Discussion

Intracardiac wall defects, such as ASDs (atrium septum defects) or VSDs (ventricular septum defects), represent common congenital cardiac pathologies with an incidence of 0.6% in live births [37]. Today's routine clinical treatment involves transcatheter deployment of septal occluder devices that consist of a metal framework and synthetic fabrics. The fabric materials in clinical use comprise permanent synthetic materials including polyurethane [38], expanded polytetrafluoroethylene [2], or Dacron [1] as well as

bioresorbable materials such as collagen type I [5]. These materials aim at induction of a natural foreign body response with tissue ingrowth from the defect periphery with sufficient defect coverage [3–5]. While, representing a promising concept with recent clinical success, these healing reactions are often characterized by incomplete and delayed incorporation of devices into the cardiac tissue, which results in a major risk of residual shunts, perforations, associated infections, arrhythmias, thrombus formation, friction lesions or fractures with device embolisation [1,3,5]. In addition, permanent unresorbable implants may also obstruct potential transeptal approaches for future treatment of acquired heart disease [5]. Considering that these devices are implanted into young patients with high life expectancies, the potential long-term consequences of these devices as part of a dynamically moving and growing system for the infant's cardiac development remains unknown. Importantly, these synthetic device materials lack the ability to grow with the developing infant's heart and may be potentially harmful for the recipients' cardiac development and/or later functionality. This suggests that after a defect closure and coverage by continuous layers of endogenous tissue, the synthetic implants are no longer necessary [3,5,6]. Besides stimulating the development of biodegradable frameworks [6], this has also stipulated the generation of biodegradable or even cell-seeded fabrics providing optimal remodeling surfaces. This could allow for a complete and fast incorporation of the devices into stable autologous tissue, representing a major prerequisite for the development of totally biodegradable devices, which resolve once this state has been reached.

In the attempt to develop artificial heart valves and vascular structures especially by means of tissue engineering, a plethora of biodegradable scaffold materials has been evaluated [3]. These included – among others – decellularized tissue-derived materials, synthetic/polymeric substances including electrospun scaffolds, biological-polymeric hybrid scaffolds, fibrin gels, and collagen-based scaffolds involving different cross-linking methods [39–41]. In the field of septal occluder systems, the *BioSTAR*[™] device was one of the first attempts of constructs with fully degradable fabrics, comprising slowly degradable acellular porcine intestinal collagen type I. This device has been broadly evaluated experimentally [42] and introduced into clinical practice [43–45]. In vivo, this novel type of devices demonstrated promising initial results with low perioperative complications [45] and adequate material function [43]. As a further technical advancement fully biodegradable systems – involving resorbable fabrics and frameworks were generated and evaluated in vivo. In a first pilot trial the devices demonstrated good integrity and mechanical strength up to 1 month post deployment [6]. However, also in these biodegradable fabric systems moderate to severe residual shunting at the implantation site was observed in up to 60% of cases after full degradation of the fabric post implantation [5].

In the strive for further improvements Jux et al. [3] were the first who created autologous cell-seeded devices in vitro using skin-derived fibroblastic cells onto collagen-coated fabrics. After in vivo implantation they reported more complete and firmer ingrowth of occluder devices underneath a thicker layer of young granulation tissue 1 month after delivery. In the contrary to acellular devices, the cell-seeded devices were fully covered by host tissue leaving none of the fabric or metal exposed. In spite of these promising results, Jux et al. reported device thrombogenicity as well as an extensive damage of the cytolayer during simulated delivery including cellular loss and loss of viability of >60% of the remaining cells limiting the clinical applicability of the proposed concept [3,46].

Conversely, tissue engineered living septal occluder systems could combine the advantages of biodegradable constructs with the advantages of endothelialized thromboresistant implants. In

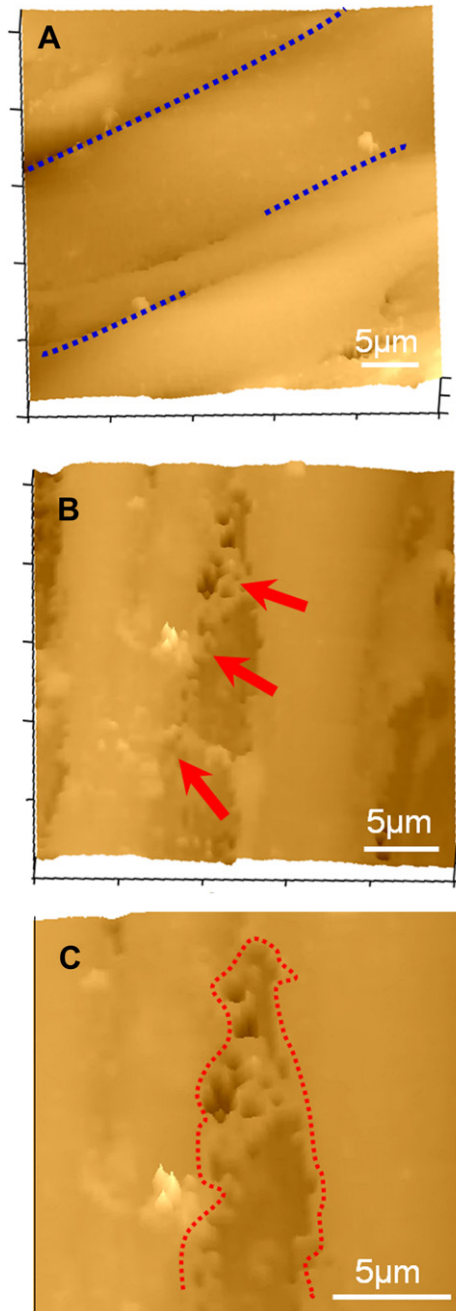


Fig. 9. Scanning ion conductance microscopy. SICM analysis revealed no detectable changes on the surface of endothelialized constructs after minor manipulation. Only after severe mechanical manipulation of the constructs involving compression by metallic devices, destructive effects on the cell margins of endothelial layers were detectable when comparing pre- (A) and post-manipulation (B–C).

addition, these bioengineered membranes may represent robust constructs providing native-like mechanical properties as well as an optimal healing environment composed of autologous vascular cells. Although this concept seems favorable, the mechanical, morphological and cellular integrity of TEOM constructs during the crimping procedure, as an essential part of the occluder delivery, seems indispensable for the future clinical realization of the concept. In the presented investigation crimping analysis and simulated delivery of TEOMs was performed revealing no detectable changes in histology, SEM, cell number (DNA) and collagen levels (HYP). Also the viability of cells did not decrease significantly during crimping and simulated delivery as indicated by live-dead analysis. Although the HYP/ μg level increased during crimping, this most likely represented an artifact of the mechanical compaction evident during the intense crimping procedure as indicated by histology. Morphological changes of the endothelial cells after crimping could be identified in SCIM analysis only when applying crimping conditions using direct mechanical manipulation usually not evident in an implantation scenario. However, this still suggests that the endothelial coverage of tissue engineered occluder membranes represents the weakest part of the constructs being potentially prone to laceration during crimping and delivery.

5. Conclusions

Here, we present the in vitro fabrication, crimping and experimental delivery of living autologous human umbilical cord-cell derived TEOMs based on PGA-P4HB composite matrices as a potential future autologous therapy of intracardiac wall defects. Future experimental in vivo studies are mandatory and will have to evaluate the clinical feasibility of the presented technology with regards to long-term defect closure and safety.

Conflict of interest statement

S P H is scientific advisor of the Xeltis AG, Switzerland.

Acknowledgments

This work was supported by the Swiss Government [EX25-2010], the Swiss National Science Foundation [32-122273], the 7th Framework Programme, Life Valve, European Commission [242008], the Centre d'Imagerie BioMedicale (CIBM) of the UNIL, UNIGE, HUG, CHUV, EPFL as well as by the Leenaards and Jeantet Foundations. The authors thank Réne Stenger, Ursula Steckholzer, Petra Wolint, Yves Wyss, Wilfried Bürzle, Klaus Marquardt, Andres Kaech (Center for Applied Microscopy and Image Analysis, University of Zurich, Switzerland), and Pia Fuchs for their support. We thank PFM Medical for providing the frameworks for the crimping analysis.

References

- Piéchaud JF. Closing down: transcatheter closure of intracardiac defects and vessel embolisations. *Heart* 2004;90(12):1505–10.
- Moake L, Ramaciotti C. Atrial septal defect treatment options. *AACN Clin Issues* 2005;16(2):252–66.
- Jux C, Bertram H, Wohlsein P, Brüggmann M, Wübaldt P, Fink C, et al. Experimental ASD closure using autologous cell-seeded interventional closure devices. *Cardiovasc Res* 2002;53(1):181–91.
- Kharouf R, Luxenberg DM, Khalid O, Abdulla R. Atrial septal defect: spectrum of care. *Pediatr Cardiol* 2008;29(2):271–80.
- Van den Branden BJ, Post MC, Plokker HW, ten Berg JM, Suttrop MJ. Patent foramen ovale closure using a bioabsorbable closure device: safety and efficacy at 6-month follow-up. *JACC Cardiovasc Interv* 2010;3(9):968–73.
- Duong-Hong D, Tang YD, Wu W, Venkatraman SS, Boey F, Lim J, et al. Fully biodegradable septal defect occluders - a double umbrella design. *Catheter Cardiovasc Interv* 2010;76(5):711–8.
- Weber B, Emmert MY, Schoenauer R, Brokopp C, Baumgartner L, Hoerstrup SP. Tissue engineering on matrix: future of autologous tissue replacement. *Semin Immunopathol* 2011;33(3):307–15.
- Schmidt D, Stock UA, Hoerstrup SP. Tissue engineering of heart valves using decellularized xenogeneic or polymeric starter matrices. *Philos Trans R Soc Lond B Biol Sci* 2007;362(1484):1505–12.
- Mol A, Rutten MC, Driessen NJ, Bouten CV, Zünd G, Baaijens FP, et al. Autologous human tissue-engineered heart valves: prospects for systemic application. *Circulation* 2006;114(1):1152–8.
- Mol A, Smits AL, Bouten CV, Baaijens FP. Tissue engineering of heart valves: advances and current challenges. *Expert Rev Med Devices* 2009;6(3):259–75.
- Mol A, Driessen NJ, Rutten MC, Hoerstrup SP, Bouten CV, Baaijens FP. Tissue engineering of human heart valve leaflets: a novel bioreactor for a strain-based conditioning approach. *Ann Biomed Eng* 2005;33(12):1778–88.
- Driessen NJ, Mol A, Bouten CV, Baaijens FP. Modeling the mechanics of tissue-engineered human heart valve leaflets. *J Biomech* 2007;40(2):325–34.
- Hoerstrup SP, Cummings I, Lachat M, Schoen FJ, Jenni R, Leschka S, et al. Functional growth in tissue-engineered living, vascular grafts: follow-up at 100 weeks in a large animal model. *Circulation* 2006;114(1):1159–66.
- Roh JD, Sawh-Martinez R, Brennan MP, Jay SM, Devine L, Rao DA, et al. Tissue-engineered vascular grafts transform into mature blood vessels via an inflammation-mediated process of vascular remodeling. *Proc Natl Acad Sci U S A* 2010;107(10):4669–74.
- Naito Y, Shinoka T, Duncan D, Hibino N, Solomon D, Cleary M, et al. Vascular tissue engineering: towards the next generation vascular grafts. *Adv Drug Deliv Rev* 2011;63(5):312–23.
- Schmidt D, Dijkman PE, Driessen-Mol A, Stenger R, Mariani C, Puolakka A, et al. Minimally-invasive implantation of living tissue engineered heart valves: a comprehensive approach from autologous vascular cells to stem cells. *J Am Coll Cardiol* 2010;56(6):510–20.
- Weber B, Scherman J, Emmert MY, Gruenenfelder J, Verbeek R, Bracher M, et al. Injectable living marrow stromal cell-based autologous tissue engineered heart valves: first experiences with a one-step intervention in primates. *Eur Heart J*; 2011 [Epub ahead of print].
- Shinoka T, Breuer C. Tissue-engineered blood vessels in pediatric cardiac surgery. *Yale J Biol Med* 2008;81(4):161–6.
- Hibino N, McGillicuddy E, Matsumura G, Ichihara Y, Naito Y, Breuer C, et al. Late-term results of tissue-engineered vascular grafts in humans. *J Thorac Cardiovasc Surg* 2010;139(2):431–6.
- Schmidt D, Mol A, Breyman C, Achermann J, Odermatt B, Gössi M. Living autologous heart valves engineered from human prenatally harvested progenitors. *Circulation* 2006;114(1):1125–31.
- Schmidt D, Achermann J, Odermatt B, Breyman C, Mol A, Genoni M, et al. Prenatally fabricated autologous human living heart valves based on amniotic fluid derived progenitor cells as single cell source. *Circulation* 2007;116(11):164–70.
- Schmidt D, Achermann J, Odermatt B, Genoni M, Zund G, Hoerstrup SP. Cryopreserved amniotic fluid-derived cells: a lifelong autologous fetal stem cell source for heart valve tissue engineering. *J Heart Valve Dis* 2008;17(4):446–55.
- Schmidt D, Breyman C, Weber A, Guenter CI, Neuenschwander S, Zund G, et al. Umbilical cord blood derived endothelial progenitor cells for tissue engineering of vascular grafts. *Ann Thorac Surg* 2004;78(6):2094–8.
- Schmidt D, Mol A, Neuenschwander S, Breyman C, Gössi M, Zund G, et al. Living patches engineered from human umbilical cord derived fibroblasts and endothelial progenitor cells. *Eur J Cardiothorac Surg* 2005;27(5):795–800.
- Schmidt D, Asmis LM, Odermatt B, Kelm J, Breyman C, Gössi M, et al. Engineered living blood vessels: functional endothelia generated from human umbilical cord-derived progenitors. *Ann Thorac Surg* 2006;82(4):1465–71.
- Schmidt D, Mol A, Odermatt B, Neuenschwander S, Breyman C, Gössi M, et al. Engineering of biologically active living heart valve leaflets using human umbilical cord-derived progenitor cells. *Tissue Eng* 2006;12(11):3223–32.
- Weber B, Zeisberger SM, Hoerstrup SP. Prenatally harvested cells for cardiovascular tissue engineering: fabrication of autologous implants prior to birth. *Placenta*; 2011 [Epub ahead of print].
- Mol A, van Lieshout MI, Dam-de Veen CG, Neuenschwander S, Hoerstrup SP, Baaijens FP, et al. Fibrin as a cell carrier in cardiovascular tissue engineering applications. *Biomaterials* 2005;26:3113–21.
- McDonald SA, Marone F, Hintermüller C, Mikuljan G, David C, Pfeiffer F, et al. Advanced phase-contrast imaging using a grating interferometer. *J Synchrotron Radiat* 2009;16(4):562–72.
- Suleski TJ. Generation of Lohmann images from binary-phase Talbot array illuminators. *Appl Opt* 1997;36:4686–91.
- Weitkamp T, Diaz A, David C, Pfeiffer F, Stampanoni M, Cloetens P, et al. X-ray phase imaging with a grating interferometer. *Opt Express* 2005;13(16):6296–304.
- Cesarone CF, Bolognesi C, Santi L. Improved microfluorometric DNA determination in biological material using 33258 Hoechst. *Anal Biochem* 1979;100(1):188–97.
- Farnedale RW, Buttle DJ, Barrett AJ. Improved quantitation and discrimination of sulphated glycosaminoglycans by use of dimethylmethylene blue. *Biochim Biophys Acta* 1986;883(2):173–7.
- Huszar G, Maiocco J, Naftolin F. Monitoring of collagen and collagen fragments in chromatography of protein mixtures. *Anal Biochem* 1980;105:424–9.

- [35] Novak P, Li C, Shevchuk AI, Stepanyan R, Caldwell M, Hughes S, et al. Nano-scale live cell imaging using hopping probe ion conductance microscopy. *Nat Methods* 2009;6(4):279–81.
- [36] Shevchuk AI, Novak P, Takahashi Y, Clarke R, Miragoli M, Babakinejad B, et al. Realizing the biological and biomedical potential of nanoscale imaging using a pipette probe. *Nanomedicine (Lond)* 2011;6(3):565–75.
- [37] Hoffman JL, Kaplan S. The incidence of congenital heart disease. *J Am Coll Cardiol* 2002;39(12):1890–900.
- [38] Sideris B, Sideris E, Calachanis M, Papantoniou V, Mouloupoulos S. The immediate release patch in the correction of experimental atrial septal defects. *Catheter Cardiovasc Interv* 2010;76(4):572–7.
- [39] Weber B, Hoerstrup SP. Regenerating heart valves. In: Cohen IS, Gaudette GR, editors. *Regenerating the heart: stem cells and the cardiovascular system*. Springer; 2011. p. 403–42 [Chapter 29].
- [40] Klouda L, Vaz CM, Mol A, Baaijens FP, Bouten CV. Effect of biomimetic conditions on mechanical and structural integrity of PGA/P4HB and electrospun PCL scaffolds. *J Mater Sci Mater Med* 2008;19(3):1137–44.
- [41] Balguid A, Mol A, van Marion MH, Bank RA, Bouten CV, Baaijens FP. Tailoring fiber diameter in electrospun poly(epsilon-caprolactone) scaffolds for optimal cellular infiltration in cardiovascular tissue engineering. *Tissue Eng Part A* 2009;15(2):437–44.
- [42] Jux C, Bertram H, Wohlsein P, Bruegmann M, Paul T. Interventional atrial septal defect closure using a totally bioresorbable occluder matrix: development and preclinical evaluation of the BioSTAR device. *J Am Coll Cardiol* 2006;48(1):161–9.
- [43] Mullen MJ, Hildick-Smith D, De Giovanni JV, Duke C, Hillis WS, Morrison WL, et al. BioSTAR Evaluation Study (BEST): a prospective, multicenter, phase I clinical trial to evaluate the feasibility, efficacy, and safety of the BioSTAR bioabsorbable septal repair implant for the closure of atrial-level shunts. *Circulation* 2006;114(18):1962–7.
- [44] Sigler M, Jux C. Biocompatibility of septal defect closure devices. *Heart* 2007;93(4):444–9.
- [45] Morgan G, Lee KJ, Chaturvedi R, Benson L. A biodegradable device (BioSTAR) for atrial septal defect closure in children. *Catheter Cardiovasc Interv* 2010;76(2):241–5.
- [46] Jux C, Bertram H, Wohlsein P, Bruegmann M, Fink C, Wueboldt P, et al. Experimental pre seeding of the STARFlex atrial septal occluder device with autologous cells. *J Interv Cardiol* 2001;14(3):309–12.